

Research of mechanical stresses in irradiated tin-doped silicon crystals

Igor Matyash, Irina Minailova*, Boris Serdega

Lashkarev Institute of Semiconductor Physics, National Academy of Sciences of Ukraine, pr. Nauki 41, Kiev 03028, Ukraine



ARTICLE INFO

Keywords:

Birefringence
Anisotropy
Modulation polarimetry
Residual stress
Silicon
Electron irradiation

ABSTRACT

An optical method of registration of mechanical stresses in undoped and tin-doped silicon samples is offered. Influence of electron irradiation on energy 5 MeV and high-temperature treatment at a 723 K on residual stresses in a silicon lattice was analyzed in the paper. The proposed method is based on a modulation of polarization of laser radiation transmitted through the anisotropic area and the definition of its anisotropy parameters by means of this modulation. The modulation polarimetry technique is an express method with high detection and resolution. The method allows identifying residual stresses in samples in absolute units with a resolution of $1 \cdot 10^{-4}$ MPa.

1. Introduction

Silicon (Si) is the basic material for numerous microelectronic, photovoltaic and sensor devices [1–4]. Its electronic properties are known to be significantly affected by the presence of impurities and defects, which play an increasingly important role with the miniaturization of devices. One of the promising silicon parameter control methods is doping by isovalent impurities [5,6]. Influence of isovalent impurities on Si properties is determined primarily by internal elastic deformations of a lattice. These deformations are due to a difference of atoms covalent radii of a matrix and impurity. Presence of local internal stresses can significantly influence on processes of defect-impurity interaction, as at a growing crystal, and under various external influences [7].

Therefore, even small changes of mechanical stresses arising in the silicon under influence of various external factors (radiation, heat treatment) [8,9], may lead to changes in electrical properties of the material. Several mechanical stress analysis techniques have been developed for silicon integrated circuits, substrate and device inspection. The most common techniques measure changes in elastic properties (e.g., micro-Raman spectroscopy, infrared grey-field polariscope, x-ray diffraction, acoustic microscopy) or stress-induced curvature of a device or structure (e.g., reflected laser, interferometry, coherent gradient sensing). Micro-Raman spectroscopy [10] is a technique for the study of local stress in silicon. It has the advantage of being non-destructive, one can control the probed depth by changing the wavelength of the exciting laser, and the spatial resolution is fairly good. Several studies are going on to improve this spatial resolution, for example by near-field optics, using optical fibers, or by decreasing the wavelength. One can

measure on the sample surface, or, if more information on the variation of the stress with depth is required, on a cleaved surface, as for example near trench structures. Although it takes a good instrument and some knowledge about factors that may influence the Raman peak position, such as temperature, laser stability and outlining, the technique is relatively simple. One measures the silicon Raman peak at different positions and one monitor the position of this peak. This directly provides important information on the local stress variations in the sample.

Infrared grey-field polariscope [11] has been developed to provide rapid, full-field stress analysis for infrared-transparent materials. The capabilities of this scientific tool are proven using standard sample geometries fabricated from single crystal silicon substrates and the general applicability of the instrument demonstrated on bonded devices and silicon wafer geometries. Stress resolution in silicon wafers is 0,1 MPa at wafer inspection speeds of 10 s for a 100 mm wafer. Initial applications of the infrared grey-field polariscope have shown that the tool provides improvements in defect detection and stress quantification when compared to conventional infrared transmission imaging.

X-ray diffraction [12] offers the highest sensitivity and is widely used in both industry and academia. This non-destructive, single-point technique measures changes in the crystal lattice spacing to determine residual stresses. Incredibly high strain sensitivities on the order of 10^{-8} can be obtained for large Bragg angles and sensitivity on the order of 10^{-5} – 10^{-4} is possible for angles of approximately 45° . Though highly sensitive, the small spot sizes and long inspection times render x-ray diffraction unsuited to real-time inspection in an industrial setting.

Scanning acoustic microscopy is a full-field, non-destructive technique capable of detecting changes in elastic properties of solids [13]. Compared to X-ray topography, this technique is relatively quick and

* Corresponding author.

E-mail addresses: i_matyash@ukr.net (I. Matyash), irinaminailova125@gmail.com (I. Minailova), bserdega@gmail.com (B. Serdega).

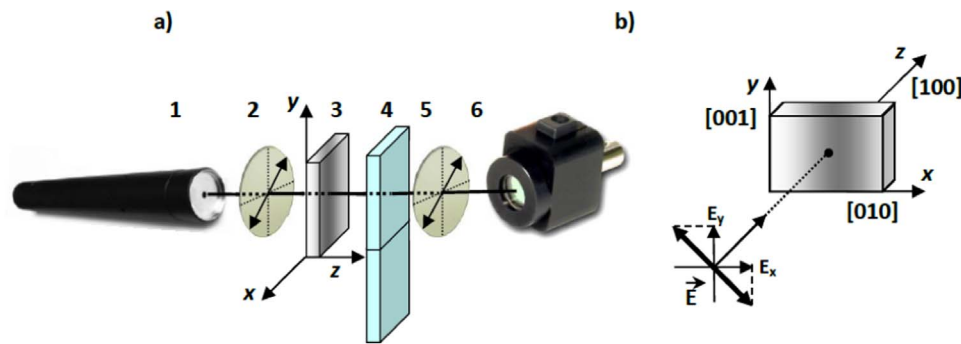


Fig. 1. The optical schema for measurements of birefringence (a): 1 – Ge-Ne laser; 2, 5 – linear polarizers; 3 – sample; 4 – photoelastic polarization modulator; 6 – photodetector; b) geometry of the experiment and crystallographic directions in the silicon crystal.

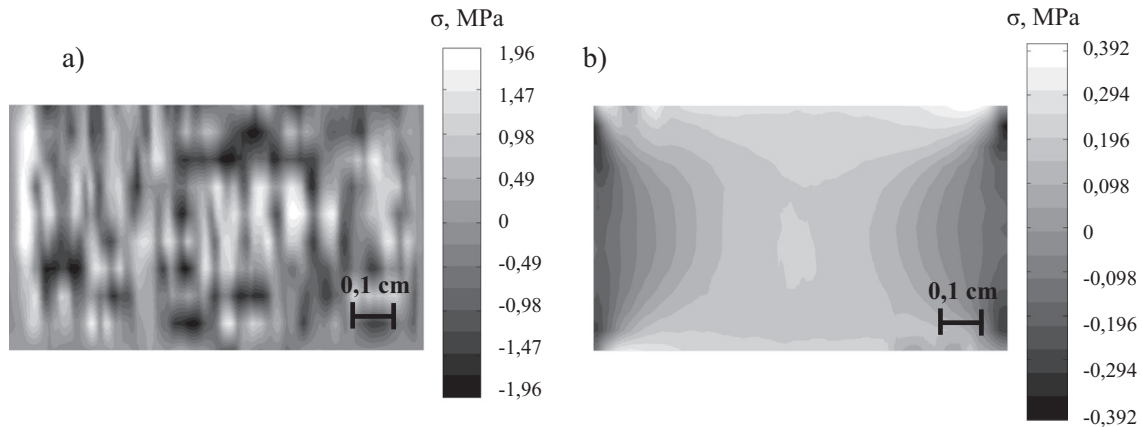


Fig. 2. Distribution of residual stresses in the tin-doped silicon sample (a); not tin-doped silicon sample (n-type) (b).

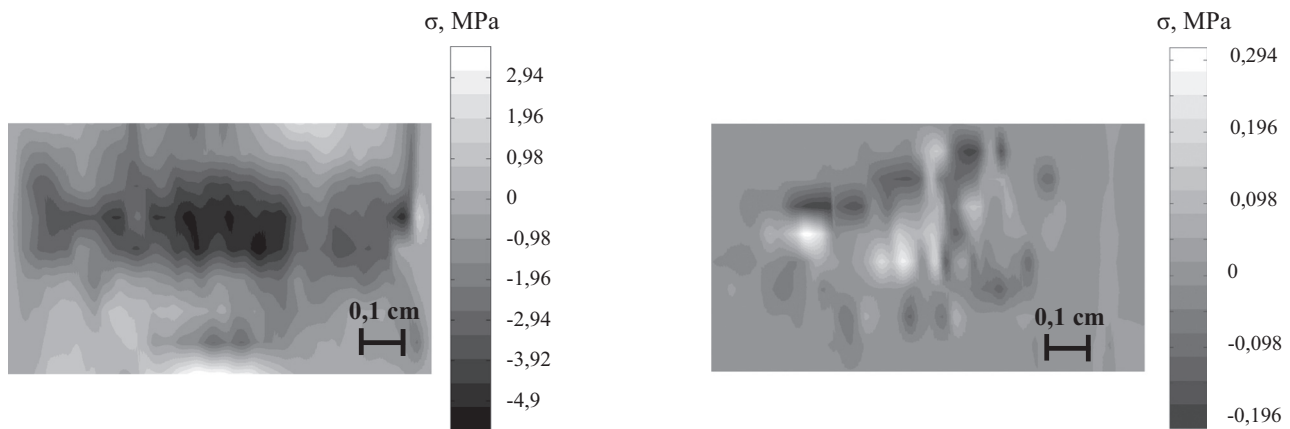


Fig. 3. Distribution of residual stresses in the tin-doped silicon sample after heat treatment at 723 K.

Fig. 4. Distribution of residual stresses in the tin-doped silicon sample after irradiation Si(Sn)_{ν} and isochronal annealing.

inexpensive and is applicable to both crystalline and amorphous materials. An important drawback of acoustic microscopy is that measurements must be carried out in a coupling liquid and the sample must be rastered in order to present two-dimensional images, again rendering this technique unsuitable to real-time, on-line inspections.

The main drawbacks of described and mentioned methods of mechanical stress registration are the following. Either the resolution is too small, or they are destructive, or they have to go hand in hand with complex modeling, or they can be applied only to a certain class of materials, or they are costly and unsuited to real-time inspection.

A technique that has shown promise for providing very sensitive residual stress measurement is photoelastic stress analysis. This method has recently evolved and is related to a category of non-destructive. However, it is not the only version of the method described in classical monographs. There is a new its version, which allows us to find low

residual stresses in Zerodur kind materials where these stresses usually considers as absent [14]. In this case, we deal with the technique of the modulation polarimetry (MP) whose detectivity is unsurpassed for registration of the birefringence caused by a directed strain. MP technique described in detail in [14–16]. The method is based on the well-established principles of photoelasticity with the addition of the polarization modulator in the optical scheme. In this article, we introduce the developed optical scheme and modulation polarimetry technique for high-precision and fast measurement of mechanical stresses in silicon samples. This method demonstrates the defect location in semiconductors using several samples (initial and after heat/radiation treatment).

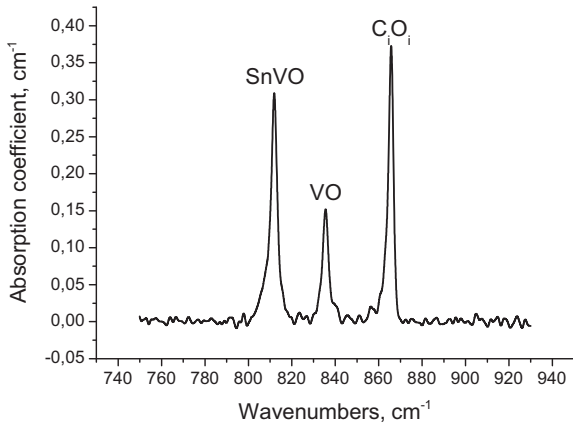


Fig. 5. Absorption spectra of irradiation silicon $\text{Si}(\text{Sn})_{ir}$ at a room temperature with dose $F_e = 5 \times 10^{17} \text{ cm}^{-2}$, $N_{\text{Sn}} = (1-2) \times 10^{19} \text{ cm}^{-3}$.

2. Material and methods

2.1. Samples

Czochralski-grown n-type Si samples doped with phosphorus, tin (Sn) and carbon were studied. The Sn concentration was $(1-2) \times 10^{19} \text{ cm}^{-3}$. All samples contained phosphorus with the concentration $(3-4) \times 10^{14} \text{ cm}^{-3}$, oxygen - $(5-6) \times 10^{17} \text{ cm}^{-3}$, carbon - $(1-1.8) \times 10^{17} \text{ cm}^{-3}$. Geometrical sizes all samples were $\sim X \times Y \times Z = 1 \times 0.6 \times 0.25 \text{ cm}$. X- and Y- coordinates of all samples were perpendicular to the growth direction of ingots [100].

The first group of $\text{Si}(\text{Sn})$ doped samples were subjected to a 40-h isochronous temperature treatment - $\text{Si}(\text{Sn})_t$ at a temperature of 723 K. Long-term temperature treatments at the 723–873 K causes the formation of oxygen precipitates (thermal donors). Samples were subjected to a 20-min annealing at an 1173 K for uniform distribution of oxygen in the sample before the temperature treatment. The second group of $\text{Si}(\text{Sn})$ doped samples were irradiated with 5-MeV electrons at a room temperature $\text{Si}(\text{Sn})_{ir}$. The dose of irradiation was $5 \times 10^{17} \text{ cm}^{-2}$. Samples were subjected to isochronal annealing at 573 K after irradiation. Annealing at temperatures $> 550 \text{ K}$ leads to a decrease of the line intensity at 836 cm^{-1} , i.e. to a decrease of V-O (vacancy - oxygen) complexes. A new line at 812 cm^{-1} appears simultaneously with a decrease of the V-O line at 836 cm^{-1} . The line at 812 cm^{-1} line is tentatively identified as related to a Sn-V-O complex, which is formed when mobile V-O centers are trapped by Sn atoms.

2.2. Physical principle of the method

The optical scheme of equipment is shown in Fig. 1a. Its operation principle the following: the radiation from Ge-Ne laser "1" ($\lambda = 1.15 \mu\text{m}$, laser beam diameter $\sim 50 \mu\text{m}$) is directed on the polarizer "2", after which the radiation became linearly polarized at an angle of 45° to X- and Y- axes (Fig. 1b). This radiation directed on the sample "3" along the Z - axis. Due to anisotropy the linearly polarized radiation is converted into elliptically polarized and is directed on the photodiode "6" through the polarization modulator "4" and polarizer "5". The elliptic polarization is a mix of linearly and circularly polarized light. The polarization modulator "4" is a special device that allows registering the intensity of only the circular (or linear) components of the elliptically polarized light.

As described above, a linearly polarized wave propagates in the Z-axis direction. The azimuth of the wave field \vec{E} is directed at an angle of 45° to the X- and Y- axes. In this case, the electric field vector \vec{E} can be decomposed into two components E_x and E_y , so they coincide with the Fresnel surface axes (optical indicatrix). Wave components after passing through the sample can obtain a phase difference $\Delta\varphi = \varphi_x - \varphi_y$

$= \frac{2\pi}{\lambda} d \cdot (n_x - n_y)$, n_x, n_y - refractive indices of the sample that depend on a magnitude and sign of stresses in the direction of corresponding axes, d - sample thickness. The phase difference $\Delta\varphi$ will increase with the increasing thickness d or sample anisotropy Δn . The phase difference $\Delta\varphi < \pi / 2$ was in our experiments. The measured signal was determined by a strict linear dependence of the difference of main components of mechanical stresses ($\sigma_x - \sigma_y$): $\Delta\phi = \frac{2\pi}{\lambda} d \cdot C \cdot (\sigma_x - \sigma_y)$, C - stress optical coefficient.

Thus, by scanning along the X- or Y-coordinate of the sample or in the fixed sample coordinate ($X = \text{const}$, $Y = \text{const}$) can be detected the birefringence distribution Δn and stress ($\sigma_x - \sigma_y$) distribution in real time. The setup allows registering a signal proportional to the value of $(\sigma_x - \sigma_y)$ in relative units. However, stress distribution is shown in absolute units. The measured signal was transferred from relative to absolute units using an additional measurement. The sample was subject to an externally controlled effort (test load). After that, the relative units of mechanical stress (birefringence units) were transferred to MPa. The resolution of setup was determined by $1 \cdot 10^{-4} \text{ MPa}$. We reiterate that the polarization method registers and measures only main components difference of mechanical stresses. The registration of shear stresses is not an object of the photoelastic effect. These stresses are not related to linearly polarized radiation and are not a research task.

3. Results and discussion

The initial tin - doped silicon samples - $\text{Si}(\text{Sn})$ was investigated. Mechanical stresses in the sample were measured. It has been found that the sample has a growth characteristic bands or bands of point defects (Fig. 2a). The positive sign of mechanical stress corresponds to compression along the OY axis, and the negative - to tension along this axis. Sign of mechanical stresses has been identified by the testing sample compression. The main sources of residual stresses in silicon are structural defects, impurities, and growth defects [17]. One of the main causes of bands of point defects can be inhomogeneity tin distribution in the ingot during growth. Bands of point defects in the crystal also may occur due to the presence of variables temperature gradients existing in the crystal during ingot growth [18]. Any deviation from the constant temperature gradient at the crystallization front causes a non-uniform thermal expansion. Such impact leads to internal stresses at a crystal solidifying [19]. Mechanical stresses were determined over the entire area of the sample and were up to 1,47 MPa.

Residual stresses of the tin - doped silicon sample - $\text{Si}(\text{Sn})$ (Fig. 2a) and not tin - doped silicon sample Si (n-type) (Fig. 2b) were compared. Si sample (Fig. 2b) was grown by Czochralski method with impurity concentration $(3-4) \cdot 10^{16} \text{ cm}^{-3}$. Fig. 2b shows a lack of bands of point defects and small residual stress to 0,39 MPa. Fig. also shows that near-surface residual stresses are significantly different from residual stresses in the silicon sample middle. Grinding and polishing of sample surfaces are a cause of this. As is known, dislocations are generated in the surface layer during mechanical treatment. Crystal lattice parameters of the surface layer have changed because of a presence of dislocations. A inconsistency of crystal lattice parameters of the surface layer and volume is a main cause of deformation. The optical anisotropy magnitude and its distribution depend on the concentration of dislocations and thickness of layer dislocations. Transmission of both samples was compared: $T_{\text{Si}} = 48\%$, $T_{\text{Si}(\text{Sn})} = 39\%$. The decrease of transmittance of the $\text{Si}(\text{Sn})$ sample, the occurrence of bands of point defects (Fig. 2a) and increased mechanical stresses can serve as confirmation of a presence of structural defects, impurities and growth defects.

Presently established that a change of electrical properties of the silicon under irradiation or heat treatment is due to a formation of stable radiation or thermal defects [9,20–22]. The presence of these defects leads to degradation of electrical and recombination parameters of silicon and determines a behavior of devices in real operating conditions.

An external influence on the crystal leads to change of defects

distribution. The consequence of this is a change of the magnitude and the coordinate dependence of mechanical stresses in the silicon crystal [23]. Formation of oxygen-containing complexes is a basic mechanism for changing of mechanical stresses. Oxygen-containing complexes are related to oxygen precipitation and occurrence of thermal donors in the silicon sample at the heat treatment [24–26]. In addition, the experimentally measured concentration of thermal donors at temperatures 623–773 K was more than theory predicts. Oxygen diffusion has activation character and increases sharply during the heat treatment of the silicon sample. Heterogeneity of oxygen distribution in silicon increases. Oxygen complexes begin to form in places with higher oxygen concentration [27,28].

Fig. 3 shows a heterogeneous distribution of residual stresses in the tin-doped silicon sample after heat treatment $\text{Si}(\text{Sn})_t$. Residual stresses in the silicon sample increased ~ 2.5 times (up to 4.9 MPa) with a decrease of transmission to $T = 34\%$. Bands of point defects are not observed. In the sample center, there is an area tension with extensive areas along the X - coordinate. Inhomogeneous distribution of intrinsic and impurity defects, their complexes [29] and accumulations of oxygen-thermal donors [30] is the explanation of this. The volume that corresponds to a silicon atom in the precipitate was larger than in the original silicon matrix. Nucleation of the precipitate accompanied by the occurrence of the field of mechanical stresses. Oxygen complexes are formed in the sample locations where the oxygen concentration is higher.

The second group of doped samples $\text{Si}(\text{Sn})$ after irradiation $\text{Si}(\text{Sn})_{ir}$ has been studied (Fig. 4). Fig. 4 shows an inhomogeneous distribution of residual stresses in the tin - doped silicon sample after irradiation $\text{Si}(\text{Sn})_{ir}$ and isochronal annealing. Residual stresses in the silicon sample reduce ~ 10 times (up to 0.29 MPa) with a decrease of transmission to $T = 20\%$. Bands of point defects hardly observed. Spectra were measured at a room temperature in the spectral range of $730\text{--}950\text{ cm}^{-1}$ using IFS-113v Fourier spectrometer with a spectral resolution of 0.5 cm^{-1} (Fig. 5).

Intensities of the absorption bands at 812 cm^{-1} corresponds to VO centers, 836 cm^{-1} - SnVO centers, 866 cm^{-1} - C_iO_i centers [31]. In our view, these radiation defects of interstitial and vacancy types lead to small residual stresses. The concentration of defects that have compression stresses is comparable to the concentration of defects that have tensile stresses in the silicon lattice. This leads to the disappearance of banding and small mechanical stresses in the sample.

Practical application of the method consists in predicting changes of residual stresses and other properties of silicon and silicon microelectronic devices when operating in conditions of high temperatures and/or high levels of ionizing radiation. We conclude that a radiation resistance of semiconductor devices is an important condition in the design of space applications systems. Since semiconductor devices must operate in outer space in conditions of severe radiation that is present in cosmic rays, solar wind and trapped in radiation belts around the Earth.

4. Conclusions

1. Modulation polarimetry technique is a very interesting and informative technique for the study of local and spatial mechanical stress in the silicon and other materials. It has the advantage of non-destructive techniques with high spatial resolution and low cost. The technique provides information about surface and internal mechanical stresses in real time.
2. The use of the offered method has shown the following:
 - Mechanical stresses in series of samples can be registered and estimated by their absolute values.
 - Identification of residual stresses is carried with a resolution of $1\cdot 10^{-4}$ MPa.
3. Thus, offered modulation polarimetry technique for determining of

mechanical stresses is a method for testing transparent solids. This diagnostic technique is particularly relevant for developers and technologists of semiconductors and semiconductor devices.

4. Practical application of the method consists in predicting changes in residual stress of the silicon and microelectronic devices during the operation in conditions of high temperatures and/or high levels of ionizing radiation.

Acknowledgements

Authors acknowledge to Dr. Khirunenko Lyudmila Ivanovna (Institute of Physics, National Academy of Sciences of Ukraine) for samples, professional advice, discussion of the experiment and support article at all stages of writing.

References

- [1] T. Hideki, Present status and prospect of Si wafers for ultra large scale integration, *Jpn. J. Appl. Phys.* 43 (7A) (2004) 4055–4067, <http://dx.doi.org/10.1143/JJAP.43.4055>.
- [2] S.W. Glunz, R. Preu, D. Biro, Crystalline silicon solar cells: state-of-the-art and future developments, in: A. Sayigh (Ed.), *Comprehensive Renewable Energy 1: Photovoltaic Solar Energy (Technology)*, Elsevier, 2012, pp. 353–387, <http://dx.doi.org/10.1016/B978-0-08-087872-0.00117-7>.
- [3] A. Bukowski, Czochralski-grown silicon crystals for microelectronics, *Acta Phys. Pol. A* 124 (2) (2013) 235–238, <http://dx.doi.org/10.12693/APhysPolA.124.235>.
- [4] H. Wang, A. Chronos, C.A. Londos, E.N. Sgourou, U. Schwingenschlogl, Carbon related defects in irradiated silicon revisited, *Sci. Rep.* 4 (2014), <http://dx.doi.org/10.1038/srep04909> (Art. no. 4909).
- [5] L.I. Khirunenko, O.O. Kobzar, Yu.V. Pomozov, M.G. Sosnin, M.O. Tripachko, Peculiarities of vacancy-related defects formation in Si doped with tin, *Physica B* 340–342 (2003) 541–545, <http://dx.doi.org/10.1016/j.physb.2003.09.139>.
- [6] L.I. Khirunenko, O.O. Kobzar, Yu.V. Pomozov, M.G. Sosnin, M.O. Tripachko, N.V. Abrosimov, H. Riemann, Interstitial-related reactions in silicon doped with isovalent impurities, *Physica B* 340–342 (2003) 546–550, <http://dx.doi.org/10.1016/j.physb.2003.09.138>.
- [7] S.M. Hu, Stress-related problems in silicon technology, *J. Appl. Phys.* 70 (6) (1991) 53–80, <http://dx.doi.org/10.1063/1.349282>.
- [8] C.A. Londos, A. Andrianakis, V.V. Emtsev, H. Ohya, Radiation-induced defects in Czochralski-grown silicon-containing carbon and germanium, *Semicond. Sci. Technol.* 24 (7) (2009) 075002, <http://dx.doi.org/10.1088/0268-1242/24/7/075002>.
- [9] L.I. Khirunenko, M.G. Sosnin, A.V. Duvanskii, N.V. Abrosimov, H. Riemann, Defects involving interstitial boron in low-temperature irradiated silicon, *Phys. Rev. B* 94 (23) (2016) 235210, <http://dx.doi.org/10.1103/PhysRevB.94.235210>.
- [10] I. De Wolf, Micro-Raman spectroscopy to study local mechanical stress in silicon integrated circuits, *Semicond. Sci. Technol.* 11 (2) (1996) 139–154, <http://dx.doi.org/10.1088/0268-1242/11/2/001>.
- [11] G. Horn, J. Lesniak, T. Mackin, B. Boyce, Infrared grey-field polariscope: a tool for rapid stress analysis in microelectronic materials and devices, *Rev. Sci. Instr.* 76 (2005) 045108, <http://dx.doi.org/10.1063/1.1884189>.
- [12] T. Vreeland, A. Dommann, C.-J. Tsai, M.-A. Nicolet, X-ray diffraction determination of stresses in thin films, *Mater. Res. Soc. Symp. Proc.* 130 (3) (1989) 3–12.
- [13] S.K. Wang, C.C. Lee, C.S. Tsai, Proceedings of the IEEE Ultrasonics Symposium, Phoenix, AZ, October 26–28, 1977, p. 171.
- [14] I. Minailova, I. Matyash, B. Serdega, V. Maslov, N. Kachur, Research on thermo-elastic tension in two-layer structure of glassceramic Zerodur by modulation polarimetry method, *Am. J. Res. Appl.* 2 (5) (2014) 93–97, <http://dx.doi.org/10.11648/j.nano.20140205>.
- [15] L.I. Berezinsky, I.L. Berezinsky, O.N. Grigorev, B.K. Serdega, V.A. Ukhimchuk, Investigation of residual stresses on the boundary of $\text{SiC}/\text{SiC} + 20\% \text{ TiB}_2$ composite materials joining by optic modulation-polarization method, *J. Eur. Ceram. Soc.* 27 (6) (2007) 2513–2519, <http://dx.doi.org/10.1016/j.jeurceramsoc.2006.08.017>.
- [16] I.E. Matyash, I.A. Minailova, B.K. Serdega, I.S. Babichuk, Research of optical and mechanical properties of lithium aluminosilicate glass-ceramics, *J. Non-Cryst. Sol.* 459 (2017) 94–98, <http://dx.doi.org/10.1016/j.jnoncrysol.2016.12.039>.
- [17] V.V. Voronkov, The mechanism of swirl defects formation in silicon, *J. Cryst. Growth* 59 (3) (1982) 625–643, [http://dx.doi.org/10.1016/0022-0248\(82\)90386-4](http://dx.doi.org/10.1016/0022-0248(82)90386-4).
- [18] T. Taishi, Y. Ohno, I. Yonenaga, K. Hoshikawa, Influence of seed/crystal interface shape on dislocation generation in Czochralski Si crystal growth, *Phys. B* 401–402 (2007) 560–563, <http://dx.doi.org/10.1016/j.physb.2007.09.021>.
- [19] T. Marek, M. Werner, P. Lavéant, G. Gerth, P. Werner, Dislocation structures in SiC films: generating “plateau-like” surface defects? *Cryst. Res. Technol.* 35 (6–7) (2000) 769–773, [http://dx.doi.org/10.1002/1521-4079\(200007\)35:6/7<769::AID-CRAT769>3.0.CO;2-S](http://dx.doi.org/10.1002/1521-4079(200007)35:6/7<769::AID-CRAT769>3.0.CO;2-S).
- [20] R. Jones, Early Stages of Oxygen Precipitation in Silicon, NATO ASI Series, Partnership Sub-Series 3 - High Technology, Kluwer Academic Publishers, Dordrecht, Netherlands, 1996, <http://dx.doi.org/10.1007/978-94-009-0355-5>.

- [21] V.P. Markevich, L.F. Makarenko, L.I. Murin, Thermal donor formation and mechanism of enhanced oxygen diffusion in silicon, in: G. Ferenczi (Ed.), *Defects in Semiconductors* 15, 38–41 1989, pp. 589–594, , <http://dx.doi.org/10.4028/www.scientific.net/MSF.38-41.589> (Mater. Sci. Forum).
- [22] S.A. McQuaid, M.J. Binns, C.A. Londos, J.H. Tucker, A.R. Brown, R.C. Newman, Oxygen loss during thermal donor formation in Czochralski silicon: new insights into oxygen diffusion mechanisms, *J. Appl. Phys.* 77 (4) (1995) 1427–1442, <http://dx.doi.org/10.1063/1.358890>.
- [23] B.K. Serdega, E.F. Venger, I.E. Matyash, The features of phonon component of linear dichroism in uniaxially strained silicon crystals, *Semicond. Phys. Quan. Electron. Optoelectron.* 6 (3) (2003) 319–323, <http://dx.doi.org/10.15407/spqeo>.
- [24] C.S. Fuller, J.A. Ditzenberger, N.B. Hannay, E. Buehler, Resistivity changes in silicon induced by heat treatment, *Phys. Rev.* 96 (3) (1954) 833, <http://dx.doi.org/10.1103/PhysRev.96.817>.
- [25] W. Kaiser, H.L. Frisch, H. Reiss, Mechanism of the formation of donor states in heat-treated silicon, *Phys. Rev.* 112 (5) (1958) 1546–1554, <http://dx.doi.org/10.1103/PhysRev.112.1546>.
- [26] P.A. Selishchev, Kinetics of production of oxygen-containing quenched-in donors in silicon and their nonuniform distribution: an analytical solution, *Semiconductor* 35 (1) (2001) 10–13, <http://dx.doi.org/10.1134/1.1340282>.
- [27] I.V. Antonova, V.P. Popov, S.S. Shaimeev, A. Misiuk, Formation of oxygen precipitates in silicon, *Semiconductor* 31 (8) (1997) 852–856, <http://dx.doi.org/10.1134/1.1187240>.
- [28] V.B. Neimash, V.M. Siratskii, A.N. Krachinskii, E.A. Puzenko, Electrical properties of silicon, heat-treated at 530 °C with subsequent electron bombardment, *Semiconductor* 32 (9) (1998) 939–943, <http://dx.doi.org/10.1134/1.1187518>.
- [29] H. Park, K.S. Jones, J.A. Slinkman, M.E. Law, The effects of strain on dopant diffusion in silicon, in: *Proceedings of IEEE International Electron Devices Meeting*, 1993, pp. 303–306, <<http://dx.doi.org/10.1109/IEDM.1993.347347>>.
- [30] A. Borghesi, B. Pivac, A. Sassella, A. Stella, Oxygen precipitation in silicon, *J. Appl. Phys.* 77 (9) (1995) 4169–4244, <http://dx.doi.org/10.1063/1.359479>.
- [31] L.I. Khirunenko, O.A. Kobzar, Yu.V. Pomozov, Defect-impurity interactions in irradiated tin-doped Cz-Si crystals, *Phys. Status Solidi (C)* 0 (2) (2003) 694–697, <http://dx.doi.org/10.1002/pssc.200306195>.